Paper 187

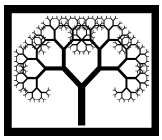

Proceedings of the Second International Conference on Railway Technology: Research, Development and Maintenance, J. Pombo, (Editor),
Civil-Comp Press, Stirlingshire, Scotland.

An Innovative Adhesion Model for Railway Applications

B. Allotta, E. Meli, L. Pugi and A. Ridolfi
Department of Industrial Engineering
University of Florence, Florence, Italy

Abstract

The accurate modelling of the adhesion plays a fundamental role in tribology, vehicle dynamics and railway systems, both from a theoretical and a practical point of view. However, a realistic adhesion law is quite difficult to obtain because of the complex and non-linear behaviour of the adhesion coefficient and the presence of external unknown contaminants; this is especially true when degraded adhesion and large sliding between the contact surfaces (for instance wheel and rail) occurs.

In this paper the authors present an adhesion model particularly developed for describing degraded adhesion conditions in vehicle dynamics and railway systems; the new approach is also quite suitable for multibody applications (very important in the considered research areas). The model analysed in this paper is based on some of the main phenomena characterising the degraded adhesion, such as large sliding at the contact interface, high energy dissipation, the consequent cleaning effect on the contact surfaces and the final adhesion recovery due to the removal of external unknown contaminants.

The adhesion model has been validated thanks to experimental data provided by Trenitalia S.p.A. coming from on-track tests performed in Velim (Czech Republic) with the railway vehicle UIC-Z1. The tests have been carried out on a straight railway track under degraded adhesion conditions with a vehicle equipped with a fully-working wheel slide protection system.

The validation highlighted the good performances of the adhesion model in terms of accuracy and numerical efficiency; in this case high computational performances are essential to implement the developed model directly online within more general multibody models (*e.g.* in Matlab-Simulink and Simpack environments). In conclusion, the adhesion model turned out to be able to well reproduce the complex phenomena behind the degraded adhesion.

Keywords: wheel-rail adhesion, degraded adhesion conditions, wheel-rail contact, multibody modelling, railway vehicles.

1 Introduction

The crucial importance of an accurate adhesion modelling in tribology, vehicular and railway applications is mainly related to its deep impact on the dynamics, the wear processes and the safety of the considered systems, both theoretically and practically. As it is well known, the adhesion coefficient shows a highly complex and non-linear behaviour, especially when degraded adhesion and large sliding between the contact surfaces occur and when external unknown contaminants are present. Therefore the modelling and the complete understanding of degraded adhesion are today important open problems.

Concerning the state of the art of the discipline and, particularly, the railway field where the multibody approaches are prevailing, the contact and adhesion models usually employed in the research activities do not consider the complex degraded adhesion behaviour and the presence of external contaminants. [1][2][3][4]

However, in the last decades, many important studies and analyses have been performed to investigate the role of the so-called third body between the contact surfaces, e.g. wheels and rails. In particular the analyses have been carried out both on laboratory test rigs and through on-track railway tests by taking into account natural and artificial external contaminants and friction modifiers. [5][6] At the same time, also the main phenomena characterizing the degraded adhesion have begun to be more accurately studied, such as large sliding at the contact interface, high energy dissipation, the consequent cleaning effect on the contact surfaces and the final adhesion recovery due to the removal of external unknown contaminants. [7][8] The model presented by the authors in this work aims to improve the accuracy in describing degraded adhesion conditions in vehicle dynamics and railway systems. Moreover the new approach has to be suitable for multibody applications (for example in Matlab - Simulink and Simpack environments), which are very important in the considered research areas. High computational performances are required so that the developed model could be directly implemented online within more general multibody models.

2 The degraded adhesion model

The main inputs of the degraded adhesion model are the wheel velocity v_w, the wheel angular velocity ω_w, the normal force at the contact interface N_c and the contact point position P_c. The model also requires the knowledge of some wheel-rail and contact parameters that will be introduced along the chapter. The outputs are the adhesion coefficient f and the tangential contact force T_c. The considered model is briefly illustrated in Figures 1 and 2 where W_{sp} is the specific energy dissipated at the contact.

Figure 1: Model inputs and outputs.

The main phenomena characterising the degraded adhesion are the large sliding occurring at the contact interface and, consequently, the high energy dissipation. Such a dissipation causes a cleaning effect on the contact surfaces and finally an adhesion recovery due to the removal of external contaminants. When the specific dissipated energy W_{sp} is low the cleaning effect is almost absent, the contaminant level h does not change and the adhesion coefficient f is equal to its original value in degraded adhesion conditions f_d. As the energy W_{sp} increases, the cleaning effect increases too, the contaminant level h becomes thinner and the adhesion coefficient f rises. In the end, for large values of W_{sp}, all the contaminant is removed (h is null) and the adhesion coefficient f reaches its maximum value f_r; the adhesion recovery due to the removal of external contaminants is now completed. At the same time if the energy dissipation begins to decrease, due for example to a lower sliding, the reverse process occurs (see Figure 2).

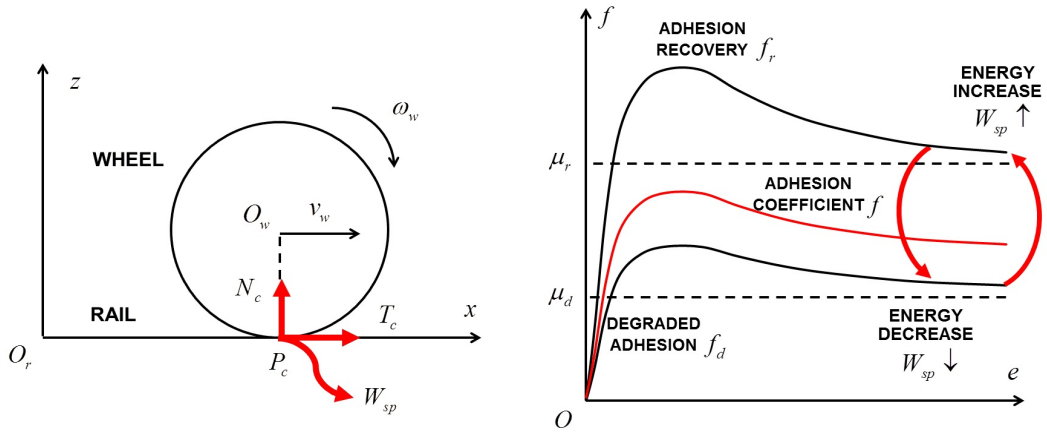

Figure 2: Behaviour of the adhesion coefficient f under degraded adhesion conditions.

Since the contaminant level h and its characteristics are usually totally unknown, it is useful trying to experimentally correlate the adhesion coefficient f directly with the specific dissipated energy W_{sp}:

$$W_{sp} = T_c e = f N_c e \quad f = T_c \setminus N_c \tag{1}$$

where the creepage e is defined as

$$e = \frac{s}{v_w} = \frac{v_w - r\omega_w}{v_w}, \tag{2}$$

s is the sliding and r is the wheel radius. This way the specific dissipated energy W_{sp} can also be interpreted as the energy dissipated at the contact for unit of distance travelled by the railway vehicle. To reproduce the qualitative trend previously described and to allow the adhesion coefficient to vary between the extreme values f_d and f_r, the following expression for f is proposed:

$$f = [1 - \lambda(W_{sp})]f_d + \lambda(W_{sp})f_r \tag{3}$$

where $\lambda(W_{sp})$ is an unknown transition function between degraded adhesion and adhesion recovery. The function $\lambda(W_{sp})$ has to be positive and monotonous increasing; moreover the following boundary conditions are supposed to be verified: $\lambda(0) = 0$ and $\lambda(+\infty) = 1$.

This way the authors suppose that the transition between degraded adhesion and adhesion recovery only depends on W_{sp}. This hypothesis is obviously only an approximation but, as it will be clearer in the next chapters, it well describes the adhesion behaviour. Initially, to catch the physical essence of the problem without introducing a large number of unmanageable and unmeasurable parameters, the authors have chosen the following simple expression for $\lambda(W_{sp})$:

$$\lambda(W_{sp}) = 1 - e^{-\tau W_{sp}} \tag{4}$$

where τ is now the only unknown parameter to be tuned on the basis of the experimental data.

In this research activity the two main adhesion coefficients f_d and f_r (degraded adhesion and adhesion recovery) have been calculated according to Polach: [1][2][6]

$$\begin{aligned} f_d &= \frac{2\mu_d}{\pi}\left[\frac{k_{ad}\varepsilon_d}{1+(k_{ad}\varepsilon_d)^2} + arctg(k_{sd}\varepsilon_d)\right] \\ f_r &= \frac{2\mu_r}{\pi}\left[\frac{k_{ar}\varepsilon_r}{1+(k_{ar}\varepsilon_r)^2} + arctg(k_{sr}\varepsilon_r)\right] \end{aligned} \tag{5}$$

where

$$\varepsilon_d = \frac{2}{3}\frac{C\pi a^2 b}{\mu_d N_c}e \quad \varepsilon_r = \frac{2}{3}\frac{C\pi a^2 b}{\mu_r N_c}e. \tag{6}$$

The quantities k_{ad}, k_{sd}, k_{ar} and k_{sr} are the Polach reduction factors (for degraded adhesion and adhesion recovery respectively) and μ_d, μ_r are the friction coefficient defined as follows

$$\mu_d = \left(\frac{\mu_{cd}}{A_d} - \mu_{cd}\right)e^{-\gamma_d s} + \mu_{cd} \quad \mu_r = \left(\frac{\mu_{cr}}{A_r} - \mu_{cr}\right)e^{-\gamma_r s} + \mu_{cr} \tag{7}$$

where μ_{cd}, μ_{cr} are the kinetic friction coefficients, A_d, A_r are the ratios between the kinetic friction coefficients and the static ones and γ_d, γ_r are the friction decrease rates. The Polach approach (see Equation 5) has been followed since it permits to describe the decrease of the adhesion coefficient with increasing creepage and to better fit the experimental data (Figure 2).

Finally it has to be noticed that the semi-axes a and b of the contact patch (see Equation 6) depend only on the normal force N_c, the material properties (the Young modulus E, the shear modulus G and the Poisson coefficient σ) and the contact point position P_c on wheel and rail (through the curvatures of the contact surfaces in the contact point) while the contact shear stiffness C (N/m^3) is a function only of the semi-axes a and b and the material properties. [4] In the end, the desired values of the adhesion coefficient f and of the tangential contact force $T_c = fN_c$ can be evaluated by solving the algebraic equation 3 in which the explicit expression of $W_{sp} = fN_c e$. Due to the simplicity of the transition function $\lambda(W_{sp})$, the solution can be easily obtained through standard non-linear solvers. [9]

3 The degraded adhesion model validation

To validate the degraded adhesion model, the new procedure has been inserted into a three-dimensional (3D) multibody model of the railway wagon UIC-Z1.

3.1 The multibody vehicle model

The degraded adhesion model has been validated by means of experimental data, provided by Trenitalia S.p.A., coming from online tests performed in Czech Republic with the UIC-Z1 coach. The considered vehicle is equipped with a fully-working wheel slide protection (WSP) system. [10]

The coach consists of one carbody, two bogie frames, eight axleboxes, and four wheelsets. The vehicle has a two-stage suspension system: the primary suspension, including springs and dampers, connects the bogie frame to four axleboxes while the secondary suspension, including springs, dampers, lateral bump-stops, anti-roll bar and traction rod, connects the carbody to the bogie frames. In Table 1 the main properties of the railway vehicle are given.

Parameter	Units	Value
Total mass	kg	43000
Wheel arrangement	-	2-2
Bogie wheelbase	m	2.56
Bogie distance	m	19
Wheel diameter	m	0.89
Primary suspension own frequency	Hz	4.5
Secondary suspension own frequency	Hz	0.8

Table 1: Properties of the railway vehicle

The wheel-rail contact model (multiple contact) includes three different steps: the detection of the contact points P_c (some innovative procedures have been recently developed by the authors in previous works [2][3]), the solution of the normal contact problem through the global Hertz theory [4] to evaluate the normal contact forces N_c and the solution of the tangential contact problem by means of the new degraded adhesion model [4][1] to compute the tangential contact forces T_c and the adhesion coefficient f. The whole vehicle model has been implemented in the Matlab-Simulink environment.

3.2 The experimental data

The experimental tests have been carried out on a straight track with the UIC-Z1 railway vehicle. The wheel profile is the ORE S1002 (with a wheelset width d_w equal to 1.5m and a wheel radius r equal to 0.445m) while the rail profile is the UIC60 (with a gauge d_r equal to 1.435m and a laying angle α_p equal to 1/20rad). In Table 2 the main wheel, rail and contact parameters are reported. [1]

Parameter	Units	Value
Young modulus E	Pa	2.1*10^11
Shear modulus G	Pa	8.0*10^10
Poisson coefficient σ	-	0.3
Polach reduction factors k_{ad}, k_{sd}	-	0.3, 0.1
Polach reduction factors k_{ar}, k_{sr}	-	1.0, 0.4
Kinetic friction coefficient μ_{cd}, μ_{cr}	-	0.06, 0.28
Friction ratios A_d, A_r	-	0.4, 0.4
Friction decrease rates γ_d, γ_r	s/m	0.2, 0.6

Table 2: Main wheel, rail and contact parameters

The value of the kinetic friction coefficient under degraded adhesion conditions μ_{cd} depends on the test that has to be performed on the track; the degraded adhesion conditions have to be reproduced using a watery solution containing surface-active agents, e. g. a solution sprinkled by a specially provided nozzle.

During the experimental campaign six different braking tests have been performed. The six tests have been split into two groups (A and B): the first group has been used to tune the degraded adhesion model (in particular the unknown parameter τ, see chapter 2, Equation 4) while the second one to properly validate the tuned model.

For each test the following physical quantities have been measured (with a sample time t_s equal to 0.01s):

1) The vehicle velocity v_v^{sp}. For the sake of simplicity all the wheel velocities v_{wj}^{sp} (j represents the j-th wheel) are considered equal to v_v^{sp};
2) The angular velocities of all the wheels ω_{wj}^{sp};
3) The vertical loads N_{wj}^{sp} on the wheels. The normal contact forces N_{cj}^{sp} can be evaluated starting from N_{wj}^{sp} by taking into account the weight of the wheels;
4) The traction or braking torques C_{wj}^{sp} applied to the wheels.

On the basis of the measured data, the experimental outputs of the degraded adhesion model, e. g. the adhesion coefficient f_j^{sp}, the tangential contact force T_{cj}^{sp} and the transition function λ_j^{sp} have now to be computed for all tests. These experimental quantities are fundamental for the model validation described in the following chapter. Equation 2 allows the calculation of s_j^{sp} and e_j^{sp} while T_{cj}^{sp} can be estimated through the rotational equilibrium of the wheel as to the origin O_w:

$$J_w \dot{\omega}_{wj}^{sp} = C_{wj}^{sp} - rT_{cj}^{sp} \tag{9}$$

in which $J_w = 160 kgm^2$ is the wheel inertia. Subsequently Equation 1 allows to calculate f_j^{sp} and the specific dissipation energy W_{spj}^{sp} while f_{dj}^{sp}, f_{rj}^{sp} can be computed directly through Equation 5. Finally, from the knowledge of W_{spj}^{sp}, f_j^{sp}, f_{dj}^{sp} and f_{dj}^{sp}, the trend of the experimental transition function $\lambda_j^{sp}(W_{spj}^{sp})$ can be determined by means of Equation 3.

3.3 The tuning of the model

During this phase of the research activity, the degraded adhesion model has been tuned on the basis of the three experimental braking tests of the group A. In particular the attention focused on the transition function $\lambda(W_{sp})$ and on the parameter τ. Starting from the experimental transition functions $\lambda_j^{sp}(W_{spj}^{sp})$ corresponding to the three tests of the group A, the parameter τ within $\lambda(W_{sp})$ has been tuned through a Non-linear Least Square Optimization (NLSO). [9] In this case the optimization process provided the optimum value $\tau = 1.9 * 10^{-4} m/J$. For instance, the comparisons between the optimized analytical transition function $\lambda(W_{sp})$ and the experimental transition function $\lambda_1^{sp}(W_{sp1}^{sp})$ is shown for the I tests of group A in Figure 3.

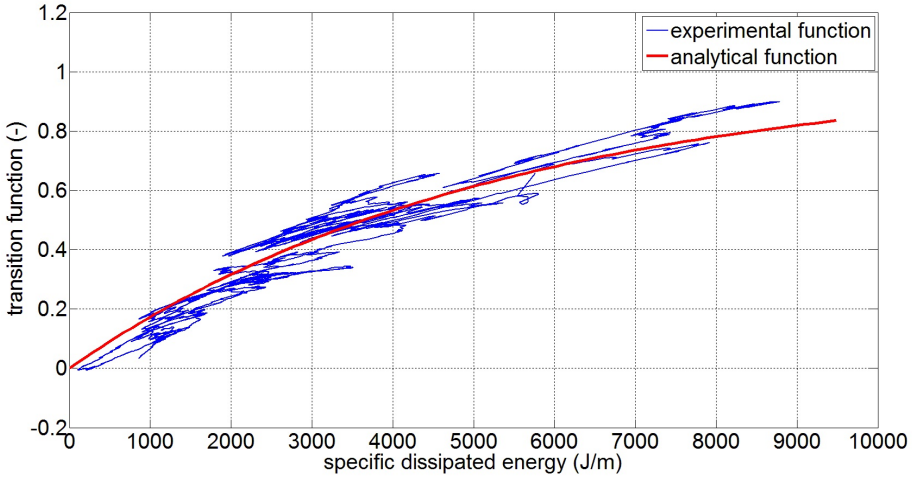

Figure 3: $\lambda(W_{sp})$ and $\lambda_1^{sp}(W_{sp1}^{sp})$, I test of group A.

In Figure 4 the time histories of the calculated and the experimental adhesion coefficients f_1, f_1^{sp} are reported for the I tests of group A.

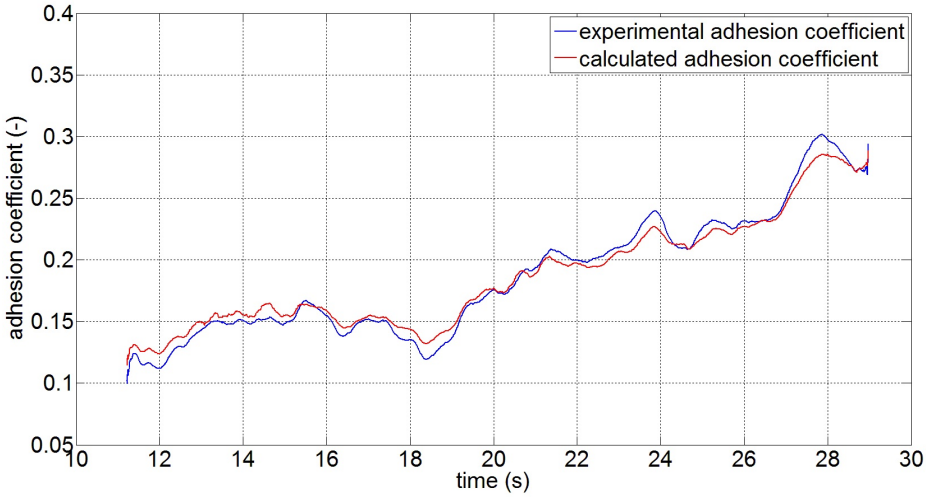

Figure 4: f_1 and f_1^{sp}, I test of group A.

By way of an example the time histories of the translational velocities v_{w1}, v_{w1}^{sp} and the rotational velocities $r\omega_{w1}$, $r\omega_{w1}^{sp}$ are reported in Figure 5 for the I test of group A (calculated and experimental).

The results of the tuning process highlight the good capability of the simple analytical transition function $\lambda(W_{sp})$ in reproducing the experimental trend of $\lambda_j^{sp}(W_{spj}^{sp})$ for all tests of group A.

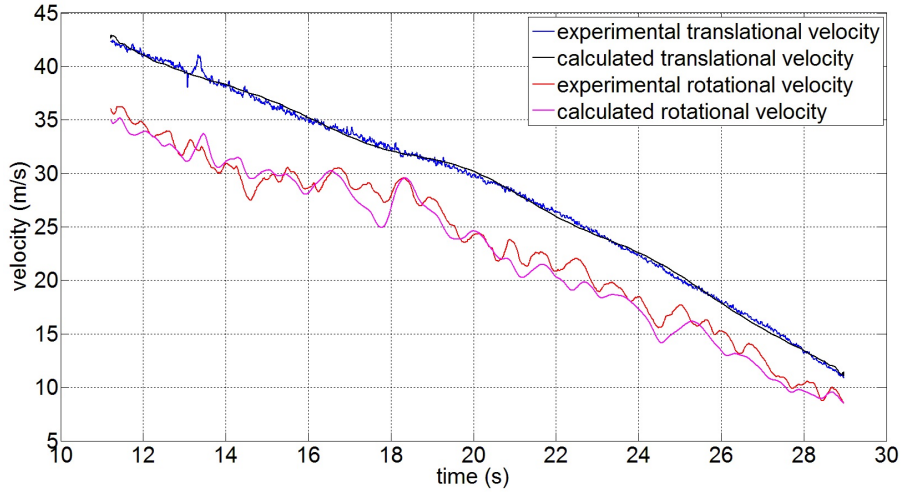

Figure 5: v_{w1}, v_{w1}^{sp} and $r\omega_{w1}, r\omega_{w1}^{sp}$, I test of group A.

The good behaviour of the analytical transition function despite its simplicity (only one unknown parameter is involved) allows also a good matching of the experimental data in terms of adhesion coefficient and velocities (especially in the second part of the braking maneuver when the adhesion recovery occurs).

3.3 The validation of the model

The real validation of the degraded adhesion model has been carried out by means of the three experimental braking tests of group B. Also in this case the attention focused first of all on the analytical transition function $\lambda(W_{sp})$ (the same tuned in paragraph 3.3 with $\tau = 1.9*10^{-4} m/J$) and on its capability in matching the behaviour of the experimental transition functions $\lambda_j^{sp}(W_{spj}^{sp})$. The comparison between $\lambda(W_{sp})$ and $\lambda_1^{sp}(W_{sp1}^{sp})$ is illustrated in Figure 6, for the I test of group B.

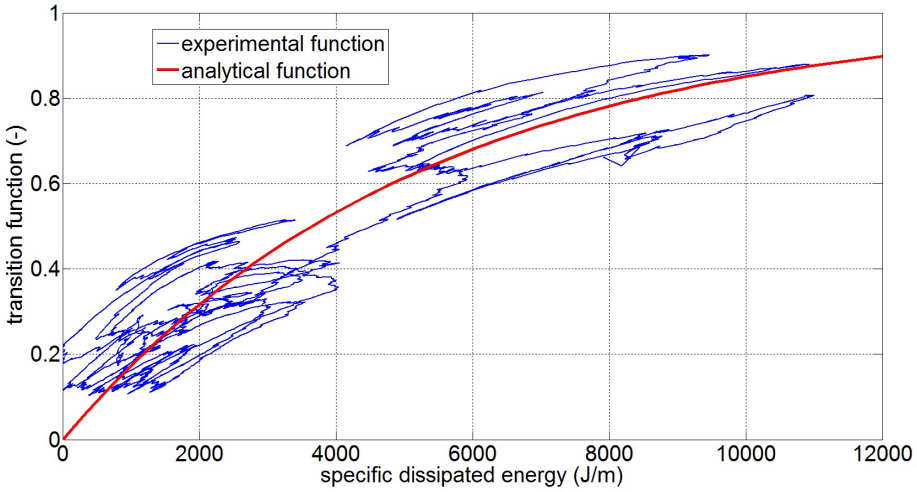

Figure 6: $\lambda(W_{sp})$ and $\lambda_1^{sp}(W_{sp1}^{sp})$, I test of group B.

The behaviour of the calculated adhesion coefficient f_j and of the experimental one f_j^{sp} have been compared again. For instance in Figure 7 the time histories of f_1, f_1^{sp} are reported for the I test of group B.

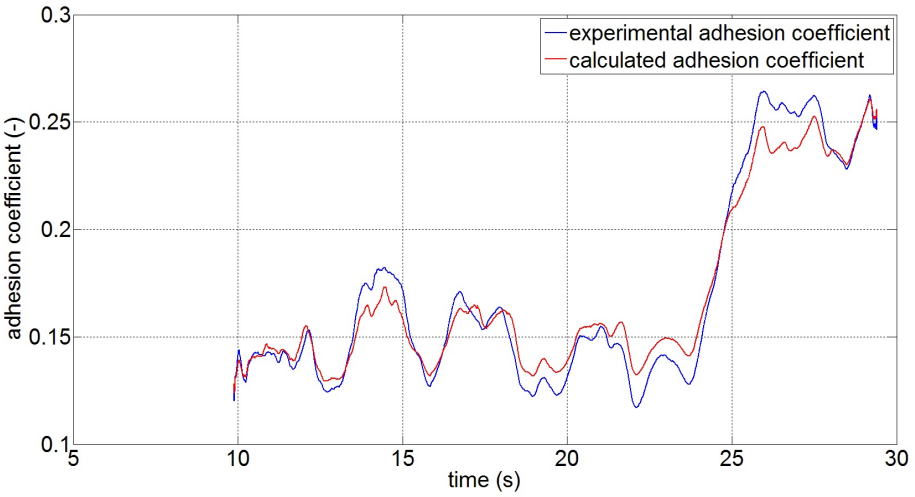

Figure 7: f_1 and f_1^{sp}, I test of group B.

Also in this case the time histories of the translational velocities v_{w1}, v_{w1}^{sp} and the rotational velocities $r\omega_{w1}$, $r\omega_{w1}^{sp}$ are reported in Figure 8 for the I test of group B (calculated and experimental).

The results of the model validation are encouraging and highlight the good matching between the analytical transition function $\lambda(W_{sp})$ (tuned in paragraph 3.3 on the basis of the tests of group A) and the new experimental data $\lambda_j^{sp}(W_{spj}^{sp})$ concerning the tests of group B.

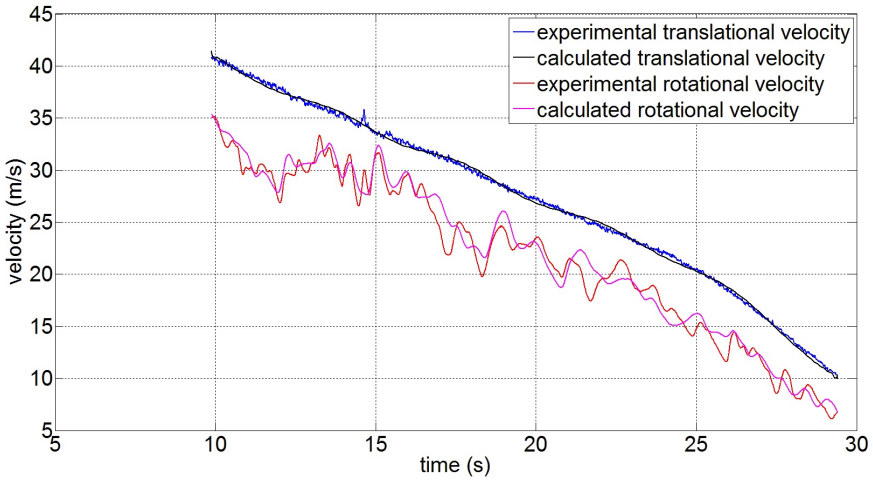

Figure 8: v_{w1}, v_{w1}^{sp} and $r\omega_{w1}, r\omega_{w1}^{sp}$, I test of group B.

At the same time, also for group B, there is a good correspondence between calculated and experimental data in terms of adhesion coefficient and velocities (especially in the second part of the braking maneuver when the adhesion recovery occurs). The satisfactory results obtained for the validation group B confirm the capability of the simple analytical transition function $\lambda(W_{sp})$ in approximating the complex and highly non-linear behaviour of the degraded adhesion.

3 Conclusions

In this work the authors presented a model aimed to obtain a better accuracy in describing degraded adhesion conditions in vehicle dynamics and railway systems. The new approach is suitable for multibody applications and assures high computational performances, making possible the direct online implementation of the degraded adhesion model within more general multibody models. The new model is based on the main phenomena characterising the degraded adhesion, such as the energy dissipation at the contact interface, the consequent cleaning effect and the resulting adhesion recovery due to the removal of external unknown contaminants. Since most of the physical characteristics of the contaminants are totally unknown in practice, the new approach minimizes the number of hardly measurable physical quantities required by the model.

References

[1] O. Polach, "Creep forces in simulations of traction vehicles running on adhesion limit", Wear, 258, 2005, 992-1000.

[2] E. Meli, S. Falomi, M. Malvezzi, A. Rindi, "Determination of wheel - rail contact points with semianalytic methods", Multibody System Dynamics, 20, 4, 2008, 327-358.

[3] J. J. Kalker, "Three-dimensional elastic bodies in rolling contact", Kluwer Academic Publisher, Netherlands, 1990.

[4] S. Falomi, M. Malvezzi, E. Meli, "Multibody modeling of railway vehicles: innovative algorithms for the detection of wheel-rail contact points", Wear, 271, 2011, 453-461.

[5] E. Nicolini, Y. Berthier, "Wheelrail adhesion: laboratory study of natural third body role on locomotives wheels and rails", Wear, 258, 2005, 1172-1178.

[6] H. Chen, T. Ban, M. Ishida, T. Nakahara, "Experimental investigation of influential factors on adhesion between wheel and rail under wet conditions", Wear, 265, 2008, 1504-1511.

[7] P. J. Blau, "Embedding wear models into friction models", Tribology Letters, 34, 2009, 75-79.

[8] R. Conti, E. Meli, L. Pugi, M. Malvezzi, F. Bartolini, B. Allotta, A. Rindi, "A numerical model of a HIL scaled roller rig for simulation of wheel-rail degraded adhesion condition", Vehicle System Dynamics, 50, 2012, 775-804.

[9] J. Nocedal, S. Wright "Numerical optimization", Springer Series in Operation Research, Berlin, Germany, 1999.

[10] B. Allotta, L. Pugi, A. Ridolfi, M. Malvezzi, A. Rindi, G. Vettori, “Evaluation of odometry algorithm performances using a railway vehicle dynamic model”, Vehicle System Dynamics 50, 2012, 699–724.